Available online at www.sciencedirect.com
ScienceDirect
Nuclear Physics B Proceedings Supplement 00 (2014) 1–7
Nuclear Physics B Proceedings Supplement

Study of $B \to K\pi\pi\gamma$ decays at the *BaBar* experiment.

Eugeni Graugés (*BaBar* collaboration)

Universitat de Barcelona. Departament d'E.C.M and ICC. Facultat de Física. Martí Franquès, 1. E-08028 Barcelona (Catalonia), Spain.

Abstract

The preliminary results obtained from the analysis of the B meson radiative decays to $K\pi\pi\gamma$, recorded at the BaBar experiment, are presented. A preliminary measurement of the time-dependent *CP* asymmetry related to the hadronic *CP* eigenstate $\rho^0 K_S^0$ is extracted from the radiative-penguin decay $B^0 \to K_S^0\pi^+\pi^-\gamma$. The decay $B^+ \to K^+\pi^+\pi^-\gamma$ is used to measure the intermediate resonant amplitudes of different resonances decaying to $K\pi\pi$ through the intermediate states $\rho^0 K^+$, $K^{*0}\pi^+$ and $(K\pi)_{\mathrm{S-wave}}\pi^+$. Assuming (isospin symmetry) that the resonant amplitudes are the same for $B^0 \to K_S^0\pi^+\pi^-\gamma$, the time-dependent *CP* asymmetry of the $B^0 \to K_S^0\rho\gamma$ decay is obtained.

Keywords: *BaBar*, PEP-II, B meson, CP violation

1. Introduction

The B meson decay into $K\pi\pi\gamma$ proceeds at leading order through a radiative (electromagnetic) penguin decay diagram, where a b quark decays into an s quark and a photon. These Flavour Changing Neutral Processes (FCNP) are forbidden within the SM at tree level, but they do occur via one-loop processes involving heavy particles (W, top). In $b \to s\gamma$ transitions, the SM predicts that B^0 ($\bar{B}^0$) decays are related predominantly to the presence of right (left) handed photons in the final state. Therefore, the mixing-induced CP asymmetry in $B \to f_{CP}$ decays, where f_{CP} is a CP eigenstate, is expected to be small. Extensions of the SM predict additional one-loop contributions where opposite helicity photons are involved and therefore can dramatically change the otherwise small SM predicted CP asymmetry. The photon polarisation itself can be accessed from the study of the angular distribution of kaonic resonance decay into three bodies $K_{res} \to K\pi\pi$ in $B \to K_{res}\gamma$, as proposed in [1] and [2], and measured by LHCb for the non-CP eigenstate $B^\pm \to K^\pm\pi^\mp\pi^\pm\gamma$ [3]. In addition, B meson decays to $K\pi\pi\gamma$ can display an interesting hadronic structure, since they have contributions from several kaonic resonances decaying to $K\pi\pi$. The decays of these resonances themselves exhibits a resonant structure, with contributions from $K^*\pi$, $K\rho$, and a $(K\pi)$ S-wave.

In this analysis, the information about the $K\pi\pi$ resonant structure is extracted by means of an amplitude analysis of the $m_{K\pi\pi}$ and $m_{K\pi}$ spectra from $B^+ \to K^+\pi^-\pi^+\gamma$ decays. The results are used, assuming isospin symmetry, to extract the mixing-induced CP parameters of the process $B^0 \to K_S^0\rho\gamma$ from the time-dependent analysis of $B^0 \to K_S^0\pi^+\pi^-\gamma$ decays without an explicit amplitude analysis of the latter mode.

The Belle collaboration has previously reported a time-dependent CP asymmetry measurement of $B^0 \to K_S^0\rho\gamma$ decays [4]. Similar measurements with $B^0 \to K_S^0\pi^0\gamma$ decays have been reported by *BaBar* [5] and Belle [6] collaborations. So far, no evidence of physics beyond the SM has been observed in these time dependent CP asymmetry measurements, which yield CP asymmetry parameters that are compatible with SM predictions. Studies of the processes $B^+ \to K^+\pi^-\pi^+\gamma$ and $B^0 \to K_S^0\pi^+\pi^-\gamma$ including measurements of the branching fractions have been performed by both *BaBar* [7] and Belle [8] collaborations. The latter also reports on the measurement of the branching fraction of the reso-

nant decay $B^+ \to K_1(1270)^+\gamma$.

2. Event reconstruction and selection.

The $B^0 \to K^0_S\pi^+\pi^-\gamma$ candidates a reconstructed from an isolated high energy photon, with a centre-of-mass (Υ(4s) rest frame) energy between 1.5 and 3.5 GeV, a pair of oppositely-charged tracks consistent with pion hypotheses and a $K^0_S \to \pi^+\pi^-$ candidate (required to have a mass within 11MeV/c^2 of the nominal K^0_S mass, and a lifetime significance of at least five standard deviations). The combinatorial background is suppressed by requiring the cosine of the angle between the K^0_S flight direction and the vector connecting the B-daughter pions and the K^0_S vertices to be greater than 0.995. For the reconstruction of the $B^+ \to K^+\pi^-\pi^+\gamma$ the K^0_S candidate is replaced by the requiring one charged track consistent with a kaon hypothesis.

A B meson candidate is kinematically characterised by the beam energy substituted mass $m_{ES} \equiv \sqrt{E^{*2}_{beam} - c^2\vec{p}^{*2}_B}/c^2$ and by the energy difference is $\Delta E \equiv E^*_B - E^*_{beam}$, where E^*_{beam} is the beam energy, and $\vec{p}^*_B$ and E^*_B are the three momentum and energy of the B candidate, respectively [1]. It is both required that $5.200 < m_{ES} < 5.292$GeV/c^2 and $|\Delta E| < 0.200$GeV/c.

To enhance discrimination between signal and continuum $q\bar{q}$ background, a Fisher discriminant [9] is used to combine six discriminating variables: the angle between the momentum of the B candidate and the beam (z) axis in the Υ(4s) rest frame, the angles between the B thrust axis and the z axis and between the B thrust axis and the thrust axis of the rest of the event, the zeroth order momentum-weighted Legendre polynomial L_0 and the ratio between the second and the zeroth order Legendre polynomials L_2/L_0 of the energy flow about the B thrust axis, and the ratio between the second and zeroth order Fox-Wolfram moments. The momentum-weighted Legendre polynomials are defined by $L_0 = \sum_i |\mathbf{p}_i|$ and $L_2 = \sum_i |\mathbf{p}_i| \frac{1}{2}\left(3\cos^2\theta_i - 1\right)$, where θ_i is the angle with respect to the B thrust axis of track or neutral cluster i and $\mathbf{p}_i$ is its momentum. The sum excludes the B candidate and all quantities are calculated in the Υ(4s) rest frame. The Fox-Wolfram moments are defined by $\mathrm{FW}(l) = \sum_{ij} |\mathbf{p}_i||\mathbf{p}_j|\mathrm{P}_l(\cos(\theta_{ij}))$, where the summation exclude the B candidate, $\mathbf{p}_i$ and $\mathbf{p}_j$ are momenta of the particles i and j, θ_{ij} is the angle between them and $\mathrm{P}_l(x)$ are the Legendre polynomials of order l. The Fisher discriminant is trained using off-resonance data for the continuum and a cocktail of exclusive simulated samples for the signal. The final sample of candidates is selected with a requirement on the Fisher discriminant that retains 90% of the signal and rejects 73% of the continuum background. Background from B decays other than the signal (B background) mainly originates from $b \to s\gamma$ processes. The exclusive B background modes are modelled and grouped into different classes that gather decays with similar kinematic and topological properties.

Background from misreconstructed π^0 and η-mesons is reduced by constructing the π^0 and η likelihood ratios, $\mathcal{LR}$, for which the photon candidate is associated with all other photons in the event. The value of $\mathcal{LR}$ is defined between zero and one, and the larger the value is, the more likely it is that the photon candidate comes from a π^0 (η) decay. The selection cut on $\mathcal{LR}_{\pi^0}(\mathcal{LR}_\eta)$, if applied before any other selection cut, retains $\sim$ 93% (95%) of signal events, while it rejects $\sim$ 83% (87%) of continuum events and $\sim$ 63% (10%) of B-background events.

3. Analysis procedure.

One of the goals of the present study is to perform a time-dependent analysis of $B^0 \to K^0_S\pi^+\pi^-\gamma$ decays to extract the direct and mixing-induced CP asymmetry parameters, $C_{K^0_S\rho\gamma}$ and $\mathcal{S}_{K^0_S\rho\gamma}$, in the $B^0 \to K^0_S\rho^0\gamma$ mode. However, due to the large natural width of the $\rho^0(770)$, a non negligible amount of $B^0 \to K^{*\pm}(K^0_S\pi^\pm)\pi^\mp\gamma$ events, which do not contribute to $\mathcal{S}_{K^0_S\rho\gamma}$, are expected to lie under the $\rho^0(770)$ resonance and dilute $\mathcal{S}_{K^0_S\rho\gamma}$. A dilution factor $\mathcal{D}_{K^0_S\rho\gamma}$ can be defined as $\mathcal{D}_{K^0_S\rho\gamma} = (\mathcal{S}_{K^0_S\pi^+\pi^-\gamma}/\mathcal{S}_{K^0_S\rho\gamma})$, where $\mathcal{S}_{K^0_S\pi^+\pi^-\gamma}$ is the effective value of the mixing-induced CP asymmetry measured for the whole $B^0 \to K^0_S\pi^+\pi^-\gamma$ dataset. Since a small number of signal events is expected in this sample, it is difficult to discriminate $B^0 \to K^{*\pm}(K^0_S\pi^\pm)\pi^\mp\gamma$ from $B^0 \to K^0_S\rho^0(\pi^\mp\pi^\pm)\gamma$ decays. Hence the dilution factor needs to be obtained by other means. To do that, the amplitudes of the different resonant modes are extracted from the charged decay channel[2] $B^+ \to K^+\pi^-\pi^+\gamma$, which has more signal events and is related to $B^0 \to K^0_S\pi^+\pi^-\gamma$ by isospin symmetry. Assuming that the resonant amplitudes are the same in both modes, the dilution factor is calculated from those of $B^+ \to K^+\pi^-\pi^+\gamma$. Moreover, the branching fractions of the different $B \to K_{\mathrm{res}}\gamma$ intermediate decay modes (where K_{res} designates a kaonic resonance decaying to $K\pi\pi$) are in general not well

[1] The asterisk denotes the Υ(4s) rest frame

[2] Charge conjugation is implicit throughout the document.

known. The amplitude analysis of the charged decay mode $B^+ \to K^+\pi^-\pi^+\gamma$ is used to extract them.

$B^+ \to K^+\pi^-\pi^+\gamma$

An unbinned extended maximum-likelihood fit to data is performed in the charged B-meson decay mode to extract the yield of $B^+ \to K^+\pi^-\pi^+\gamma$ correctly signal events. The fit uses the variables ΔE, $m_{\rm ES}$, and the Fisher-discriminant output to discriminate signal events from misreconstructed signal events, continuum background and B background. Using information from the maximum likelihood fit, the $m_{K\pi\pi}$, $m_{K\pi}$ and $m_{\pi\pi}$ spectra in signal events are extracted using the ${}_s\mathcal{P}lot$ technique [10].

A binned maximum-likelihood fit is performed to the signal ${}_s\mathcal{P}lot$ of $m_{K\pi\pi}$ in order to extract from data the branching fractions of the various kaonic resonance decaying to $K^+\pi^-\pi^+$. The $m_{K\pi\pi}$ distribution is modeled as a coherent sum of five resonances described by Relativistic Breit-Wigner (RBW) line shapes, with widths that are taken to be constant. The model is summarized in Tab. 1. Due to the fact that helicity angles are not explicitly taken into account in fit model, it only has to account for interference between resonances with same spin parity, J^P.

Table 1: The five kaonic resonances decaying to $K^+\pi^-\pi^+$ included in the model used to fit the $m_{K\pi\pi}$ spectrum. The pole mass m^0 and width Γ^0 are taken from Ref. [11].

J^P	$K_{\rm res}$	Mass m^0 (MeV/c^2)	Width Γ^0 (MeV/c^2)
1^+	$K_1(1270)$	1272 ± 7	90 ± 20
	$K_1(1400)$	1403 ± 7	174 ± 13
1^-	$K^*(1410)$	1414 ± 15	232 ± 21
	$K^*(1680)$	1717 ± 27	322 ± 110
2^+	$K_2^*(1430)$	1425.6 ± 1.5	98.5 ± 2.7

Finally a binned maximum-likelihood fit is performed to the signal ${}_s\mathcal{P}lot$ of $m_{K\pi}$ in order to extract from data the amplitudes and the branching fractions of the intermediate resonances decaying to $K^+\pi^-$ and $\pi^+\pi^-$. The choice to project the $m_{\pi\pi}$–$m_{K\pi}$ phase space of $B^+ \to K^+\pi^-\pi^+\gamma$ decays on the $m_{K\pi}$ dimension is driven by the difficulty of performing a full two-dimensional amplitude analysis with the given the event sample size. This is further complicated by the four-body nature of the decay: since the value of $m_{K\pi\pi}$ can vary from event to event, the kinematic boundaries for the $m_{\pi\pi}$–$m_{K\pi}$ plane vary as well. We model the $m_{K\pi}$ spectrum as the projection of two 1^- P-wave and one 0^+ S-wave components. The two P-wave components, namely the $K^{*0}(892)$ and the $\rho^0(770)$ resonances, are described by Relativistic Breit-Wigner and Gounaris-Sakurai (GS) line shapes, respectively. The 0^+ (S-wave) component of the $K\pi$ spectrum, designated by $(K\pi)_0$, is modeled by the LASS parameterization [12], which consists of the $K_0^*(1430)^0$ resonance together with an effective range non-resonant component. Table 2 summarizes the $m_{K\pi}$ fit model; it details the line shapes used for the three contributions and their parameters.

Both in the fit to the $m_{K\pi\pi}$ and the $m_{K\pi}$ spectra, the relative amplitudes (magnitudes and phases) of the different components of the corresponding signal model are directly measured. The amplitudes of the different kaonic resonances extracted from the fit to the $m_{K\pi\pi}$ spectrum are used to compute their relative fractions in the fit ("fit fractions"). These, in turn, are used to extract branching fractions of the different $K_{\rm res}$ contributions, that are used as inputs to the $m_{K\pi}$ fit model. The amplitudes of the three $K^+\pi^-$ and $\pi^+\pi^-$ intermediate states, extracted from the fit to the $m_{K\pi}$ spectrum, are used to compute the dilution factor. In order to optimize the sensitivity on $\mathcal{S}_{K_S^0\rho\gamma}$, when calculating the dilution factor, additional cuts on $m_{\pi\pi}$ and $m_{K\pi}$ are applied. It is required that $m_{\pi\pi} \in [0.600, 0.900](\,\mathrm{GeV}/c^2)$, in order to enhance the proportion of the $\rho^0(770)$ resonance. Similarly a veto is applied to on the $K^*(892)$ resonance requiring $m_{K\pi} \in [m_{K\pi}^{\rm min}, 0.845] \cup [0.945, m_{K\pi}^{\rm max}](\,\mathrm{GeV}/c^2)$, where $m_{K\pi}^{\rm min}$ and $m_{K\pi}^{\rm max}$ denote the allowed phase-space boundaries in the $m_{K\pi}$ dimension.

$B^0 \to K_s^0\pi^+\pi^-\gamma$

In the neutral B-meson decay mode, an unbinned extended maximum-likelihood fit to data to extract the yield of $B^0 \to K_s^0\pi^+\pi^-\gamma$ signal events is performed. Here, the additional selection cuts $0.6 < m_{\pi\pi} < 0.9\,\mathrm{GeV}/c^2$, $m_{K\pi} < 0.845\,\mathrm{GeV}/c^2$ and $m_{K\pi} > 0.945\,\mathrm{GeV}/c^2$ are applied for consistency with the corresponding requirements in the charged mode. The fit uses the variables ΔE, $m_{\rm ES}$, and the Fisher-discriminant output to discriminate signal events from continuum background and B background. The signal time-dependent decay rate is given by:

$$\mathcal{P}(\Delta t, \sigma_{\Delta t}) \equiv \frac{e^{-|\Delta t|/\tau_{B^0}}}{4\tau_{B^0}} \times \left[1 + q_{\rm tag}\frac{\Delta D^c}{2}\right.$$

$$\left. - q_{\rm tag}\,\langle D\rangle^c\, C\cos(\Delta m_d \Delta t) \;\; + q_{\rm tag}\,\langle D\rangle^c\, \mathcal{S}\sin(\Delta m_d \Delta t)\right]$$

$$\otimes\, \mathcal{R}^c(\Delta t, \sigma_{\Delta t})\,,$$

where $q_{\rm tag}$ is the flavor-tag of the event: $q_{\rm tag} = -1$ for B^0 mesons (i.e. $B_{\rm rec} = B^0$ and $B_{\rm tag} = \bar{B}^0$) and $q_{\rm tag} = +1$ for $\bar{B}^0$ mesons (i.e. $B_{\rm rec} = \bar{B}^0$ and $B_{\rm tag} = B^0$), τ_{B^0} is the B^0 lifetime and Δm_d is the $B^0\bar{B}^0$ oscillation frequency, fixed to the measurement from Ref [13]. The parameter $\langle D\rangle^c$ and ΔD^c, which are separated by the flavor and tagging category c of the tag side B decay, are related to the probability of incorrectly reporting a $B_{tag} = B^0(\bar{B}^0)$ as $\bar{B}^0$ (B^0) and to a possible difference in performance of the tagging procedure for the two tags, respectively. The resolution function in tagging category c, $\mathcal{R}^c(\Delta t, \sigma_{\Delta t})$, which is convoluted with the Δt probability density function (PDF), takes into account the imperfect measurement of Δt. The coefficients $\mathcal{S}$ and C are the parameters associated with mixing-induced *CP* violation and direct *CP* violation, respectively.

For backgrounds from charged B mesons decays, Δt is modeled as an exponential decay with an effective lifetime; while for backgrounds from neutral B mesons decays to *CP* eigenstates, we account for possible *CP* violation effects using a similar Δt PDF for signal with an effective lifetime. The continuum background Δt PDF is modeled as a combination of "prompt" decays and "lifetime" decays coming from charmed mesons. Each of the background Δt PDFs are convoluted with corresponding resolution functions.

The fit yields the direct and mixing-induced *CP* asymmetries in the whole $B^0 \to K^0_S\pi^+\pi^-\gamma$ sample, $C_{K^0_S\pi^+\pi^-\gamma}$ and $\mathcal{S}_{K^0_S\pi^+\pi^-\gamma}$. The latter is then multiplied by the dilution factor to obtain the parameter of interest, $\mathcal{S}_{K^0_S\rho\gamma}$.

Table 2: The three resonances included in the model used to fit the $m_{K\pi}$ spectrum and their line-shape parameters. The nominal mass and width of the resonance, m_0 and Γ_0, which are expressed in MeV/c^2, are taken from the references detailed in the table. The parameter r for $\rho^0(770)$ and $K^{*0}(892)$ is the Blatt-Weisskopf radius of barrier. The parameters a and r of the $(K\pi)_0$ are the scattering length and the effective range, respectively. The values of the parameters are taken from [11] and [12].

J^P	Resonance	Parameters
1^-	$K^{*0}(892)$	$m_0 = 895.94 \pm 0.22$ $\Gamma_0 = 50.8 \pm 0.9$ $r = 3.6 \pm 0.6$ (GeV/c)$^{-1}$
	$\rho^0(770)$	$m_0 = 775.49 \pm 0.34$ $\Gamma_0 = 149.1 \pm 0.8$ $r = 5.3^{+0.9}_{-0.7}$ (GeV/c)$^{-1}$
0^+	$(K\pi)_0$	$m_0 = 1425 \pm 50$ $\Gamma_0 = 270 \pm 80$ $a = 2.07 \pm 0.10$ (GeV/c)$^{-1}$ $r = 3.32 \pm 0.34$ (GeV/c)$^{-1}$

4. Results

In the charged B-meson decay mode, the maximum-likelihood fit to data results in $2441 \pm 91^{+34}_{-57}$ signal $B^+ \to K^+\pi^-\pi^+\gamma$ events, where the first quoted uncertainty is statistical and the second is systematic. The extracted ${}_s\mathcal{P}lot$ distribution for $m_{K\pi\pi}$ is shown in Fig. 1, and the branching fractions of the kaonic resonances, which are extracted from the fit to this $m_{K\pi\pi}$ distribution itself, are given in Tab. 3.

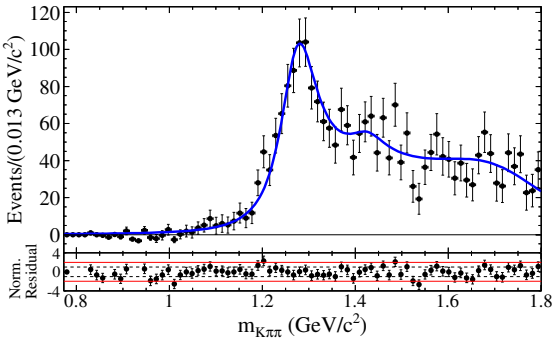

Figure 1: Distribution of $m_{K\pi\pi}$ for $B^+ \to K^+\pi^-\pi^+\gamma$ signal events (${}_s\mathcal{P}lot$), extracted from the maximum likelihood fit to $m_{\rm ES}$, ΔE, and the Fisher discriminant. Points with error bars give the sum of ${}_s$Weights. The blue solid curve is the result of the fit performed directly to this $m_{K\pi\pi}$ distribution to extract the different contributions from kaonic resonances decaying to $K^+\pi^-\pi^+$. Below each bin are shown the residuals, normalized in error units. The parallel dotted and full lines mark the one and two standard deviation levels, respectively.

Figure 2 shows the $m_{K\pi}$ ${}_s\mathcal{P}lot$ distribution that is, like the $m_{K\pi\pi}$ spectrum, extracted from the maximum likelihood fit to $m_{\rm ES}$, ΔE, and the Fisher discriminant. The figure also shows the contributions of the different intermediate resonances, as extracted from the fit to the $m_{K\pi}$ spectrum itself. The relative magnitudes and phases of the different components of the signal model are measured directly from this fit. From these quantities we extract the branching fractions, summarized in Tab. 4, and compute the dilution factor. The dilution factor measured to be $\mathcal{D}_{K^0_S\rho\gamma} = 0.549^{+0.096}_{-0.094}$, where the quoted uncertainties are sums in quadrature of statistical and systematic uncertainties.

In the neutral B-meson decay mode, the maximum-likelihood fit to data yields $245 \pm 24^{+13}_{-16}$ signal $B^0 \to K^0_S\pi^+\pi^-\gamma$ events. This results in an inclusive branching

Table 3: Branching fractions of the different kaonic resonance ($K_{\rm res}$) decaying to $K^+\pi^-\pi^+$, extracted from the fit to the $m_{K\pi\pi}$ spectrum. The quoted numbers are averaged over charge-conjugate states. They are obtained using the "fit fraction" of each component and the corresponding efficiency. To correct for the secondary branching fractions we use the values from Ref. [11]. The first uncertainty is statistical, the second is systematic, and the third, when present, is due to the uncertainties on the secondary branching fractions.

Mode	$\mathcal{B}(B^+ \to \text{Mode}) \times \mathcal{B}(K_{\rm res} \to K^+\pi^+\pi^-) \times 10^{-6}$	$\mathcal{B}(B^+ \to \text{Mode}) \times 10^{-6}$	PDG values ($\times 10^{-6}$)
$B^+ \to K^+\pi^+\pi^-\gamma$	$\cdots$	$27.2 \pm 1.0^{+1.1}_{-1.3}$	27.6 ± 2.2
$K_1(1270)^+\gamma$	$14.5^{+2.0+1.1}_{-1.3-1.2}$	$44.0^{+6.0+3.5}_{-4.0-3.7} \pm 4.6$	43 ± 13
$K_1(1400)^+\gamma$	$4.1^{+1.9+1.3}_{-1.2-0.8}$	$9.7^{+4.6+3.1}_{-2.9-1.8} \pm 0.6$	< 15 CL= 90%
$K^*(1410)^+\gamma$	$9.7^{+2.1+2.4}_{-1.9-0.7}$	$23.8^{+5.2+5.9}_{-4.6-1.4} \pm 2.4$	$\emptyset$
$K_2^*(1430)^+\gamma$	$1.5^{+1.2+0.9}_{-1.0-1.4}$	$10.4^{+8.7+6.3}_{-7.0-9.9} \pm 0.5$	14 ± 4
$K^*(1680)^+\gamma$	$17.0^{+1.7+3.5}_{-1.4-3.0}$	$71.7^{+7.2+15}_{-5.7-13} \pm 5.8$	< 1900 CL= 90%

Table 4: Branching fractions of the different resonances decaying to $K\pi$ and $\pi\pi$, extracted from the fit to the $m_{K\pi}$ spectrum. The quoted numbers are averaged over charge-conjugate states. They are obtained using the "fit fraction" of each component and the corresponding efficiency. R denotes an intermediate resonant state and h stands for a final state hadron: a charged pion or kaon. To correct for the secondary branching fractions we used the values from Ref. [11] and $\mathcal{B}(K^{*0}(892) \to K^+\pi^-) = \frac{2}{3}$. The first uncertainty is statistical, the second is systematic, and the third, when applicable, is due to the uncertainties on the secondary branching fractions. The last two rows of the table are obtained by separating the contributions from the resonant and the non-resonant part of the LASS parametrization.

Mode	$\mathcal{B}(B^+ \to \text{Mode}) \times \mathcal{B}(R \to hh) \times 10^{-6}$	$\mathcal{B}(B^+ \to \text{Mode}) \times 10^{-6}$	PDG values ($\times 10^{-6}$)
$B^+ \to K^+\pi^+\pi^-\gamma$	$\cdots$	$27.2 \pm 1.0^{+1.1}_{-1.3}$	27.6 ± 2.2
$K^{*0}(892)\pi^+\gamma$	$17.3 \pm 0.9^{+1.2}_{-1.1}$	$26.0^{+1.4}_{-1.3} \pm 1.8$	20^{+7}_{-6}
$K^+\rho(770)^0\gamma$	$9.1^{+0.8}_{-0.7} \pm 1.3$	$9.2^{+0.8}_{-0.7} \pm 1.3 \pm 0.02$	< 20 CL= 90%
$(K\pi)_0^{*0}\pi^+\gamma$	$11.3 \pm 1.5^{+2.0}_{-2.6}$	$\cdots$	$\emptyset$
$(K\pi)_0^0\pi^+\gamma$ (NR)	$\cdots$	$10.8^{+1.4+1.9}_{-1.5-2.5}$	< 9.2 CL= 90%
$K_0^*(1430)^0\pi^+\gamma$	$0.51 \pm 0.07^{+0.09}_{-0.12}$	$0.82 \pm 0.11^{+0.15}_{-0.19} \pm 0.08$	$\emptyset$

fraction of $\mathcal{B}(B^0 \to K^0\,\pi^+\,\pi^-\,\gamma) = (23.9 \pm 2.4^{+1.6}_{-1.9}) \times 10^{-6}$. In both cases, the first quoted uncertainty is statistical and the second is systematic. The result of the fit to data for the time-dependent *CP* violation parameters in signal events is

$$\mathcal{S}_{K^0_S\pi^+\pi^-\gamma} = 0.14 \pm 0.25(\text{stat.})^{+0.04}_{-0.03}(\text{syst.}) ,$$
$$C_{K^0_S\pi^+\pi^-\gamma} = -0.39 \pm 0.20(\text{stat.}) \pm 0.05(\text{syst.}) .$$

In order to obtain the value of $\mathcal{S}_{K^0_S\rho\gamma}$, we divide $\mathcal{S}_{K^0_S\pi^+\pi^-\gamma}$

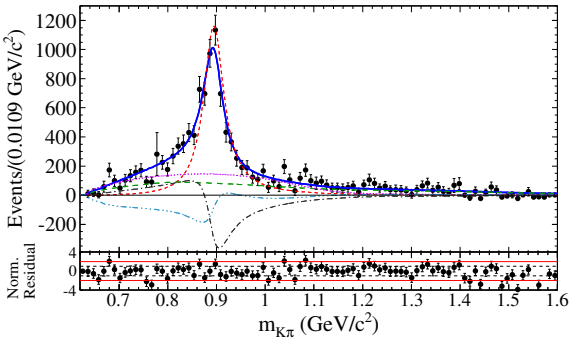

Figure 2: Distribution of $m_{K\pi}$ for $B^+ \to K^+\pi^-\pi^+\gamma$ signal events ($_s\mathcal{P}lot$), extracted from the maximum likelihood fit to $m_{\rm ES}$, ΔE, and the Fisher discriminant. Points with error bars give the sum of $_s$Weights. The blue solid curve is the result of the fit performed directly to this $m_{K\pi}$ distribution to extract the different contributions from $K\pi$ and $\pi\pi$ intermediate states. The small-dashed red, medium-dashed green and dotted magenta curves correspond to the $K^{*0}(892)$, $\rho^0(770)$ and $(K\pi)$ S-wave contributions, respectively. The dashed-dotted gray curve corresponds to the interferences between the two P-wave components, i.e. the $K^{*0}(892)$ and the $\rho^0(770)$, while the dashed-triple-dotted light blue curve corresponds to the interferences between the $(K\pi)$ S-wave and the $\rho^0(770)$. Below each bin are shown the residuals, normalized in error units. The parallel dotted and full lines mark the one and two standard deviation levels, respectively.

by the dilution factor given in Eq. 4 and obtain

$$\mathcal{S}_{K^0_S\rho\gamma} = 0.25 \pm 0.46(\text{stat.})^{+0.08}_{-0.06}(\text{syst.})\,.$$

4.1. Systematic uncertainties

In the $B^+ \to K^+\pi^-\pi^+\gamma$ decay analysis, various sources of systematic uncertainties affecting the amplitudes extracted from the fits to the $m_{K\pi\pi}$ and the $m_{K\pi}$ spectra were considered. These were propagated to the dilution factor and the different branching fractions deduced from the amplitudes.

Among sources of systematic uncertainties on the $K_{\rm res}$ amplitudes extracted from the fit to the $m_{K\pi\pi}$ spectrum, we account for effects from the fixed parameters in the maximum-likelihood fit to $m_{\rm ES}$, ΔE and the Fisher discriminant, the fixed line-shape parameters of the kaonic resonances in the fit model, the effects of adding kaonic resonances at high masses to the fit model, the procedure of the signal $m_{K\pi\pi}$ $_s\mathcal{P}lot$ extraction, as well as the number of bins in the fitted distribution, are all accounted for. The dominant systematic uncertainty originates from the fixed line-shape parameters of the resonances.

The amplitudes extracted from the fit to the $m_{K\pi}$ spectrum are found to be affected, among other minor sources, by the fixed parameters in the maximum-likelihood fit to $m_{\rm ES}$, ΔE and the Fisher discriminant, the fixed line-shape parameters of the resonances in the fit model, the weights of the kaonic resonances used to construct the total PDF (extracted from the fit to the $m_{K\pi\pi}$ spectrum), the line-shape parameters of the kaonic resonances used in the simulation generator, the number of bins in the fitted distribution, the number of bins in histogram PDFs, as well as the procedure of the signal $m_{K\pi}$ $_s\mathcal{P}lot$ extraction. Here, the dominant source of systematic uncertainty is due to the weights of the kaonic resonances.

Specific sources of systematic uncertainties are also taken into account for the extraction of branching fractions. Namely, the uncertainties on the number of $B\bar{B}$ pairs recorded in the full *BABAR* dataset, input branching fractions, tracking efficiency, photon reconstruction and selection efficiency, and $K^\pm$ and $\pi^\pm$ particle identification.

In the analysis of $B^0 \to K^0_S\pi^+\pi^-\gamma$ decays, systematic uncertainties affecting the inclusive branching fraction and the *CP*-violation parameters are studied. In order to assign systematic uncertainties due to the fixed parameters in the maximum likelihood fit to $m_{\rm ES}$, ΔE, the Fisher discriminant, and Δt each of the fixed parameters are varied within its uncertainties, and repeat the fit. Also, the systematic uncertainties on the dilution factor are propagated to $\mathcal{S}_{K^0_S\rho\gamma}$.

In addition to the specific sources of systematic uncertainties on branching fractions accounted for in the analysis of $B^+ \to K^+\pi^-\pi^+\gamma$ decays, the uncertainties due to the K^0_S selection are also taken into account.

5. Conclusion

A preliminary measurement of the time-dependent *CP* asymmetry in the radiative-penguin decay $B^0 \to K^0_S\pi^+\pi^-\gamma$, using a sample of 470.9 million $\Upsilon(4S) \to B\bar{B}$ events recorded with the *BABAR* detector at the PEP-II e^+e^- storage ring at SLAC, has been presented. Using events with $m_{K\pi\pi} < 1.8\,\text{GeV}/c^2$, $0.6 < m_{\pi\pi} < 0.9\,\text{GeV}/c^2$ and with $m_{K\pi} < 0.845\,\text{GeV}/c^2$ and $m_{K\pi} > 0.945\,\text{GeV}/c^2$, the *CP*-violating parameters $\mathcal{S}_{K^0_S\pi^+\pi^-\gamma} = 0.14 \pm 0.25^{+0.04}_{-0.03}$ and $C_{K^0_S\pi^+\pi^-\gamma} = -0.39 \pm 0.20 \pm 0.05$, are obtained. From this measurement the time-dependent *CP* asymmetry related to the hadronic *CP* eigenstate $\rho^0K^0_S$ is extracted to be $\mathcal{S}_{K^0_S\rho\gamma} = 0.25 \pm 0.46^{+0.08}_{-0.06}$. This observable provides information on the photon polarization in the underlying $b \to s\gamma$ transition. To extract $\mathcal{S}_{K^0_S\rho\gamma}$ from $\mathcal{S}_{K^0_S\pi^+\pi^-\gamma}$, assuming isospin symmetry, we study $B^+ \to K^+\pi^+\pi^-\gamma$ decays and measure intermediate resonant amplitudes of different resonances decaying to $K\pi\pi$ through the in-

termediate states $\rho^0 K^+$, $K^{*0}\pi^+$ and $(K\pi)_{\mathrm{S-wave}}\pi^+$. In addition to the need of this information for the extraction of $\mathcal{S}_{K^0_S\rho\gamma}$, it provides input on the $K\pi\pi$ system, which is useful for other studies of the photon polarization. The branching fractions of the different $K_{\mathrm{res}} \to K\pi\pi$ states as well as the overall branching fractions of the $\rho^0 K^+$, $K^{*0}\pi^+$ and $(K\pi)_{\mathrm{S-wave}}\pi^+$ components have also been measured.

References

[1] M. Gronau, Y. Grossman and A. Ryd, *Phys. Rev. Lett.* **88**, 051802, 2002
[2] M. Gronau and D. Pirjol, *Phys. Rev. D* **66**, 054008, 2002
[3] LHCb collaboration, *Phys. Rev. Lett.* **112**, 161801, 2014
[4] Belle collaboration, *Phys.Rev.Lett.*, **101**, 251601, 2008.
[5] *BaBar* collaboration, *Phys.Rev.*, D **78**, 071102, 2008.
[6] Belle collaboration, Ushiroda, *Phys.Rev.*, D **74**, 111104, 2006.
[7] *BaBaR* collaboration, *Phys.Rev.Lett.*, **98**, 211804, 2007.
[8] Belle collaboration, *Phys.Rev.Lett.*, **94**,111802, 2005.
[9] R. A. Fisher, *Annals Eugen.*, **7**, 179-188, 1936.
[10] M. Pivk, F. R. Le Diberder, *Nucl. Instrum. Meth.*, **A555**:356, 2005.
[11] Particle Data Group collaboration, *Phys. Rev.*, **D86**:010001, 2012
[12] LASS collaboration, *Nucl. Phys.* , **B296**:493, 1988
[13] *BaBaR* collaboration, *Phys.Rev.Lett.*, **99**,171803, 2007.